Analyzing the Performance of Integrated Collector Storage Solar Water Heater using Neuronal Approach

Djamel Hassani [1*], Hamid Abdi[2], Salah Hanini , Kamel Daoud

[1] LBMPT, University of Medea, Algeria; [2] 2E2D, University of Blida, Algeria

(Corresponding Author): *Email: djamelhassani@hotmail.com

Received: 21-04-2023 **Accepted:** 12-08-2023 **Published:** 17-08-2023

Abstract

One way to directly benefit from solar energy is through solar thermal systems that produce hot water. These systems function similarly to greenhouses, where sun rays are absorbed by absorbers and then used to reheat fluid that flows through a heating device. Ongoing research aims to improve the efficiency of these systems to achieve more effective models. A news method for data processing and modeling is the neural method, which operates similarly to biological neural networks. This technique allows for accurate models with a minimal number of parameters and can process even nonlinear and multivariable phenomena by learning from representative experimental data. This work aims to develop a strategy based on artificial neural networks to calculate the relevant parameters of a solar system and characterize a solar water heater, specifically focusing on the self-storage sensor that converts sunlight into thermal energy. By embracing the potential of neural networks in solar technology, this initiative not only seeks to refine parameter calculations but also to elevate the overall operational performance of solar water heaters, contributing to the ongoing advancement of sustainable energy solutions.

Keywords: Solar energy; Self storage sensor; Artificial neural networks; Modelling; Approximation.

Tob Regul Sci. ™ 2023;9(1): 4458-4469
DOI: doi.org/10.18001/TRS.9.1.313

1. Introduction

One method of utilizing solar energy directly is through the production of hot water using heat sensors, which convert sunlight into heat energy. Ongoing research is being conducted to improve the efficiency of these devices through the development of more efficient models. Previous studies have focused on the use of neural methods for predicting, optimizing, and characterizing the performance of solar energy systems. For example, Kalogirou et al. [1] reported the use of an ANN model for estimating the performance of a thermosiphon solar water heater, while Kalogirou [2] utilized an ANN model and genetic algorithms for the optimization of solar systems. Additionally, ANN has been used for predicting flat-plate collector performance parameters by Kalogirou [3], determining the effectiveness of a plan solar sensor by Sözen et al. [4], and developing a diagnostic system for solar water heaters based on ANN by Kalogirou et al. [5]. Souliotis et al. [6] presented a combination of an appropriate ANN and TRNSYS for predicting the performance of an Integrated Collector Storage (ICS) prototype. Esen et al. [7] used both ANN and wavelet neural network (WNN) models to model a new solar air heater (SAH) system.

The neuronal approach is a novel modeling technique that offers several advantages over traditional methods as it does not rely on explicit knowledge of physical laws. This approach is particularly useful for dealing with nonlinear phenomena and multivariable systems, as it can be configured through learning from representative experimental data. The objective of this study is to develop a strategy based on artificial neural networks to optimize the important parameters of a solar self-storage water heater with a reflector. The reflector serves to concentrate sunlight on the probe's surface and can also act as an insulating jacket to minimize heat loss during nighttime.

2. Solar energy in southern Algeria

Despite its strategic geographical location, Algeria has failed to fully capitalize on the potential of solar energy, as its utilization has remained stagnant for more than forty years. However, Figure 1 illustrates that Algeria boasts one of the largest solar fields globally.

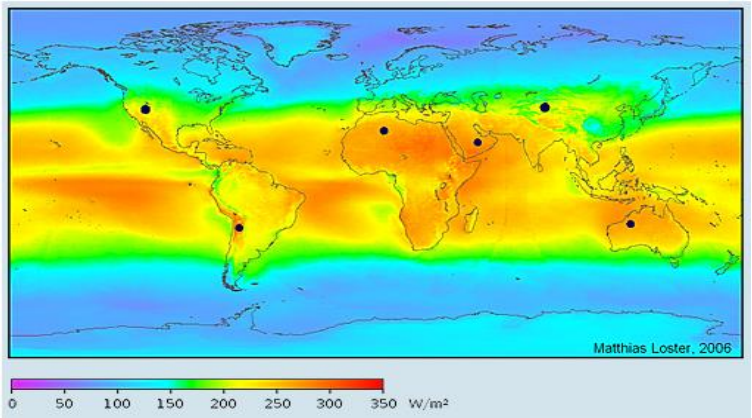

Figure 1. Map of the average sunlight received on the ground in the world.

The amount of sunshine in the region exceeds 2000 hours per year, and can even reach 3900 hours in highlands and Sahara (Fig. 2). According to Boudries et al. [8], the daily solar energy received on a 1m^2 horizontal area is approximately 5kWh throughout the country. The annual solar energy received is around 1700kWh/m^2 in the North and 2263kWh/m^2 in the South, as stated by MEM [9]. Due to the long distances between communities and the scattered population in the Sahara, the use of renewable energy is crucial for sustainable development in southern Algeria, as it significantly reduces the expensive cost of power lines.

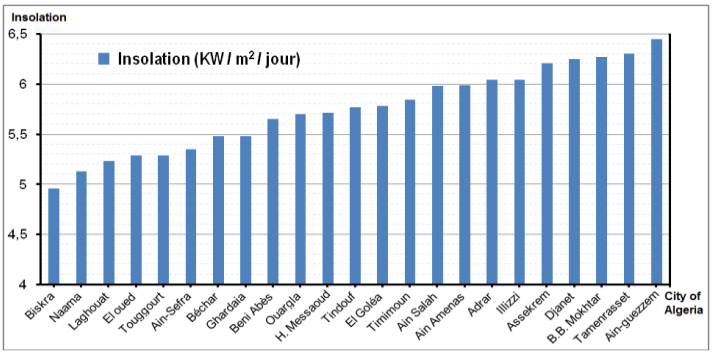

Figure 2. Solar Potential in Algerian Sahara [8].

3. Thermal sensor

The assessment of a solar system's thermal performance relies on mathematical models derived from a heat balance and measurements carried out according to established standards. The most commonly used model for flat plate collectors is the Hottel-Whillis-Bliss (HWB) model, which was developed in 1959 by Bliss [10]. Various standards have been created, such as ASHRAE Standard 93-77 by the American Society of Heating in 1978 [11]. However, these standards, which are based on quasi-stationary heat balance, are not appropriate for sensor self-storage due to the large heat capacity of water stored in the sensor element storekeeper. The relaxation time of the sensors self-storage is in the range of several hours, making it impossible to achieve a quasi-stationary regime during testing in the external environment [12, 13].

In the existing literature, there are few studies specifically focused on characterizing sensors self-storage. Typically, this characterization is based on experimental measurements of the temperature of the collector surface. Authors usually employ mathematical models that assume uniform storage temperature, resulting in a discrepancy between the experimental and calculated results. To address this issue, we propose a non-conventional modeling approach that utilizes a technique not dependent on explicit knowledge of physical laws but instead requires numerical data.

4. Presentation of solar sensor

H. Abdi conducted an experimental study of the solar system at the experimental station of solar equipment in rural Saharian of Adrar, located in the south of Algeria. The coordinates of the site are latitude 27.88°; longitude - 0.17° W; and it is situated 264m above sea level with an albedo of 0.2 [14].

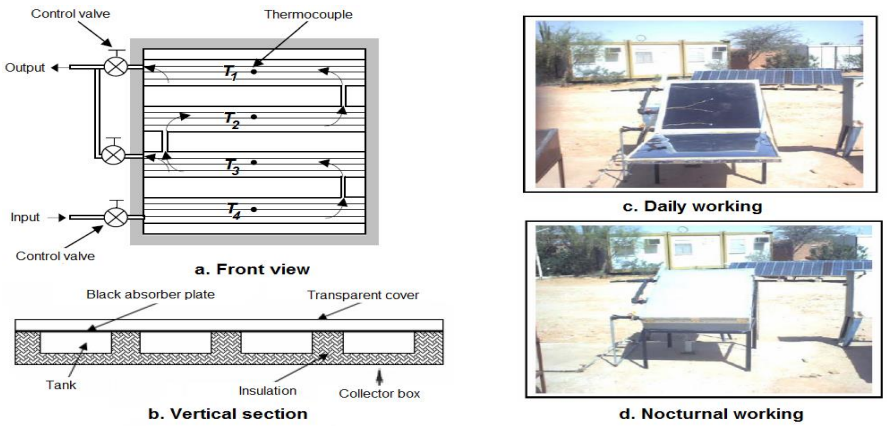

Figure 3. Experimental setup [14].

Figure 3 showcases the design of the sensor-storer solar system, which consists of four tanks connected together and equipped with a reflector. The prototype is constructed using galvanized steel sheets, with each tank open on the side exposed to solar radiation. The sensor-storer, also made of galvanized steel, is placed inside the tank. To minimize heat loss and create a greenhouse effect, the tank is

covered with glass. Additionally, the sensor is equipped with a reflector that concentrates solar radiation on the collector surface and acts as an insulating blanket to reduce heat loss at night.
Temperature measurements in the room (T_a) and water storage tanks (T_1, T_2, T_3, and T_4) are recorded using type K thermocouples (Chromel / Alumel). These thermocouples are connected to a Hydra Data Acquisition Unit (Model 2620 A), which has 20 channels for data recording. The global irradiance is measured using a pyranometer.

The sensor-storer undergoes three test series:

1. In the first series of tests, the sensor operates with a reflector and insulation applied before use. During daily tests, the insulating blanket is placed on the sensor at 4:30 pm and removed the next day at 8:00 am.
2. In the second series of tests, the sensor operates with a reflector but without front insulation.
3. In the third series of tests, the sensor operates without reflectors and front insulation.

5. Artificial neural network model

The concept of artificial neural networks draws inspiration from the way biological neurons handle information. It is applied to develop software simulations that involve interconnected processing elements in a parallel manner. In a similar fashion to how dendrites of biological neurons receive electrochemical impulses from other neurons, artificial neurons in these networks receive analogous inputs. Consequently, artificial neural networks can be seen as a collection of processing elements and weighted connections resembling a network of neurons.

The arrangement of artificial neurons in layers (Fig. 4a) involves the input layer receiving inputs (s_i) from the real world. Each subsequent layer then receives weighted outputs ($w_{ij}.s_i$) from the previous layer as its input, creating a feed forward artificial neural network (ANN). In this type of network, each input is passed forward to the next layer where it is processed. The outputs of the final layer serve as the outputs to the real world. Neurons in hidden or output layers in a feed forward ANN have two main functions: they calculate the sum of weighted inputs from multiple connections and a bias value, and then apply a transfer function to this sum. They also transmit the resulting value through outgoing connections to the neurons of the following layer, where the same process occurs.

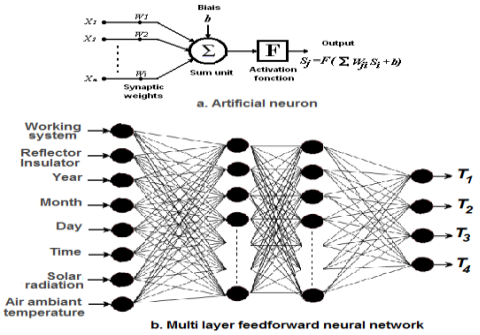

Figure 4. Representation of neuron formal and Multi-layer feed forward neural network for the prediction of the four temperatures of tanks.

The calculation of the output is accomplished using a transfer function, also referred to as an activation function. It is preferable for this activation function to exhibit a step-like behavior. Additionally, as optimization algorithms necessitate continuity and differentiability at all points, certain characteristics outlined in previous research by Hassani et al. [15, 16] and Si-moussa et al. [17] are desired.

The number of neurons in the input and output layers is determined by the count of independent and dependent variables, respectively. The user defines both the number of hidden layers and the quantity of neurons contained within each hidden layer. The construction of the model involves a training process, during which a collection of experimental data related to independent variables is presented to the network's input layer. The resulting outputs from the output layer constitute predictions for the dependent variables within the model. The network learns the connections between the independent and dependent variables by iteratively comparing projected outputs with experimental results. Subsequent adjustments to the weight matrix and bias vector of each layer are performed through a back propagation training algorithm. Consequently, the network constructs a neural network model capable of reasonably accurate predictions for output variables within the model's defined space, as established by the training dataset. As such, the primary aim of ANN modeling is to minimize prediction errors for validation data introduced to the network after the training phase concludes.

While ongoing discussions regarding model selection strategies persist, it is evident that the effective utilization of ANN for engineering problems' modeling is significantly influenced by four main factors:

1. Network type,
2. Network structure (number of hidden layers, quantity of neurons per hidden layer),
3. Activation functions,
4. Training algorithms.

It's well established that varying the number of neurons in the hidden layer(s) significantly impacts the predictive ability of the network. The most common approach for optimizing ANN performance is to adjust the numbers of neurons in the hidden layer(s) and select the architecture that demonstrates the highest predictive ability [15, 16, 17].

The design and optimization of the ANN were conducted through three primary stages. Initially, essential parameters such as transfer functions and training functions were tested in the first stage. Subsequently, in the second stage, various pre-processing methods were assessed to identify the most suitable one for the network. Finally, the third stage involved fine-tuning the network by determining the optimal number of hidden layers and neurons in each layer.

In Figure 4b, we can observe the architecture of the utilized Artificial Neural Network (ANN) designed to predict the temperatures of tanks. This ANN is composed of four layers, including an input layer, two hidden layers, and an output layer. The input layer incorporates all the relevant input

factors, which undergo processing through the two hidden layers. Eventually, the output layer generates the output vector.

In Table 1, a comprehensive overview of the neural networks developed for temperature prediction in the tanks is presented. The table includes essential information such as the learning algorithm, the number of hidden layers, the number of neurons in each hidden layer, and the activation function employed in the respective networks.

Table 1. Characteristics of neural networks developed for the prediction of the four temperatures of tanks

Type of network	Multi-layer feed forward neural network	
Layer	**Number of neurons**	**Activation function**
Input layer	8	
First hidden layer	18	Hyperbolic tangent sigmoid
Second hidden layer	18	Hyperbolic tangent sigmoid
Output layer	4	Linear
Training Algorithm	BRBP using Levenberg–Marquardt optimization	

Figures 5 to 8 display the performance of the neural network model for predicting the first temperature (T_1), the second temperature (T_2), the third temperature (T_3) and the fourth temperature (T_4). The correlation coefficients for these temperature predictions are 0.997, 0.998, 0.998 and 0.996 respectively.

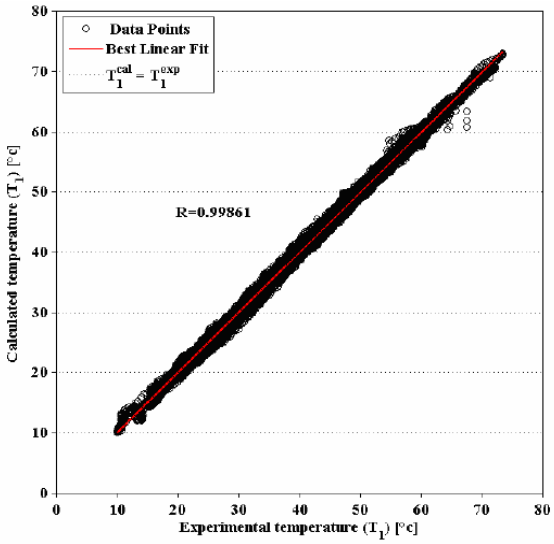

Figure 5. Performance of ANN to calculate the first temperature (T_1).

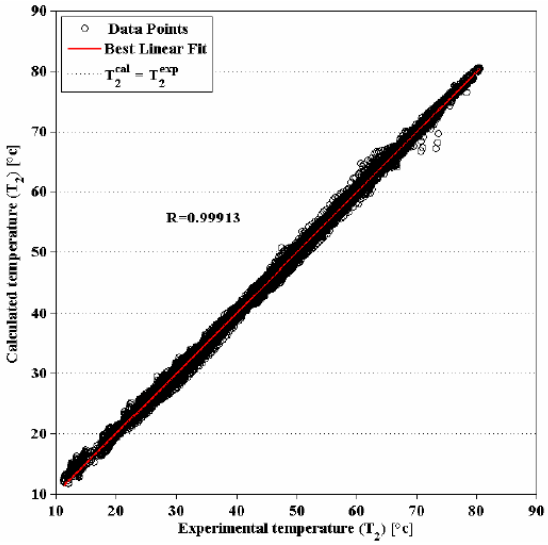

Figure 6. Performance of ANN to calculate the second temperature (T_2).

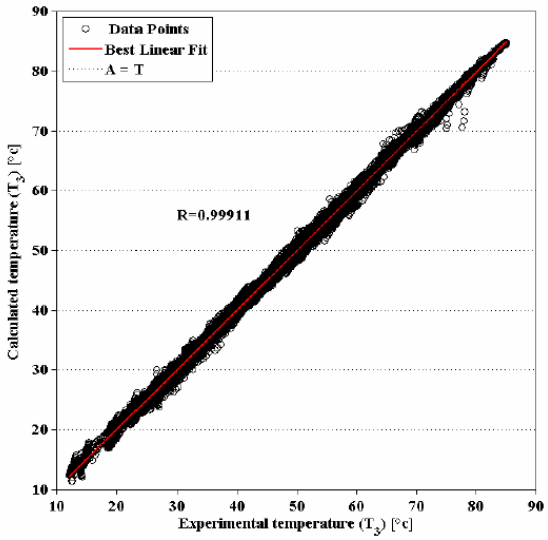

Figure 7. Performance of ANN to calculate the third temperature (T_3).

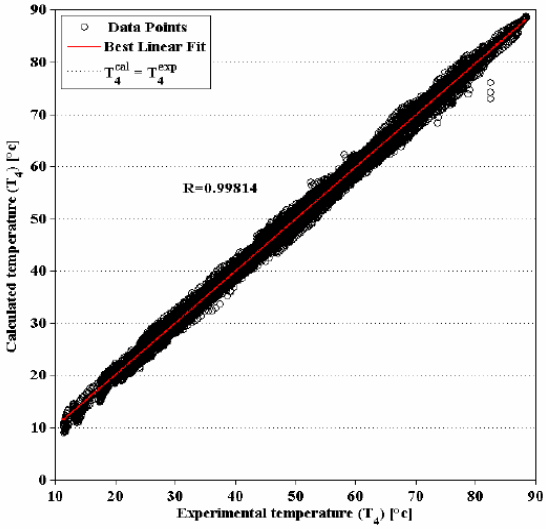

Figure 8. Performance of ANN to calculate the fourth temperature (T_4)

Table 2 presents the commonly used deviations calculated for the four predicted outputs of the ANN model (T_1, T_2, T_3, and T_4) across the entire dataset:

Average Absolute Relative Deviation:

$$AARDT_i(\%) = \frac{100}{n}\sum_{i=1}^{n}\left|\frac{T^{\exp} - T^{cal}}{T^{\exp}}\right| \quad (1)$$

Average Square Relative Deviation:

$$ASRDT_i(\%) = \frac{100}{n}\sum_{i=1}^{n}\left(\frac{T^{\exp} - T^{cal}}{T^{\exp}}\right)^2 \quad (2)$$

Average Absolute Deviation:

$$AADT_i = \frac{1}{n}\sum_{i=1}^{n}\left|T^{\exp} - T^{cal}\right| \quad (3)$$

Table 2. Statistical analyses of the error of the predicted results

Systems		AARDT$_i$ (%)	ASRDT$_i$ (%)	AADT$_i$
System 1	T_1	1.115	0.023	0.530
	T_2	0.861	0.014	0.460
	T_3	0.862	0.015	0.482
	T_4	1.421	0.035	0.798
System 2	T_1	1.401	0.036	0.452
	T_2	1.068	0.024	0.383
	T_3	1.125	0.026	0.428
	T_4	1.698	0.055	0.653
System 3	T_1	1.559	0.055	0.435
	T_2	1.184	0.039	0.360
	T_3	1.113	0.033	0.376
	T_4	1.827	0.073	0.624

6. Experimental and neuronal characterization

In this section, the results obtained from the ANN were utilized to determine the optical and thermal characteristics of solar water heating systems (ICSSWH). These results were then compared and contrasted with the experimental characterization.

For the characterization of the sensor, the mathematical model developed by David Faiman [12, 13] was adopted. This model introduces the concept of Maximum Useful Efficiency (MUE), aiming to derive an algebraic expression similar to that proposed by Hottel-Whillier-Bliss [10], but with the distinction that the variables represent average values rather than instantaneous ones. The Maximum Useful Efficiency is defined by the following equation:

$$\eta = \overline{K} F_E \eta_o - F_E U_L \left(\overline{T_f} - \overline{T_a}\right) / \overline{I} \qquad (4)$$

In Equation (4), the symbols represent the following variables: T_f represents the temperature of the water in storage, T_a denotes the room temperature, and I represents the irradiance on the aperture plane of the collector. η_o is the optical efficiency of the collector, while U_L represents the heat loss coefficient of the collector-storage unit. K is the incidence angle modifier, and F_E is an enthalpy retrieval factor defined as:

$$F_E = \frac{M_w C_w}{M_w C_w + M_{cs} C_{cs}} \qquad (5)$$

Where: M_w and C_w are respectively the mass and heat capacity of the water. M_{cs} and C_{cs} are the respective mass and heat capacity of the material from which the collector-storage unit is fabricated.

The bars in Equation 4 indicate average values over the daily heating period, from sunrise until the time the water reaches its maximum daily temperature. The maximum useful efficiency (η) is defined as the ratio between the maximum energy extracted by the fluid and the incident energy on the sensor plane:

$$\eta = \frac{M_w C_w \left(T_{\max} - T_{sunrise}\right)}{A_c \int I(t) dt} \qquad (6)$$

In the evaluation of Equation (4), the collector aperture area (A_c) is taken into account, and the integral is computed over the time interval from sunrise until the water reaches its maximum temperature. The results obtained by applying Equation (4) are depicted in Figures 9 to 12.

Figures 9 and 10 illustrate the thermal performance variation of the sensor for both systems: one without a reflector and the other with a reflector. It is evident that the thermal efficiency of the sensor is significantly improved when equipped with a reflector, as indicated by the results obtained from the experimental and neural methods.

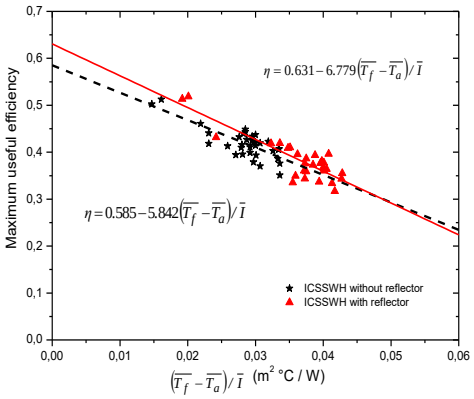

Figure 9. Characteristic graph of ICSSWH using experimental temperatures.

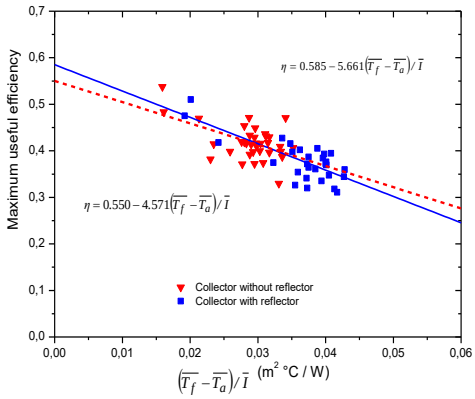

Figure 10. Characteristic graph of ICSSWH using predicted temperatures ANN model.

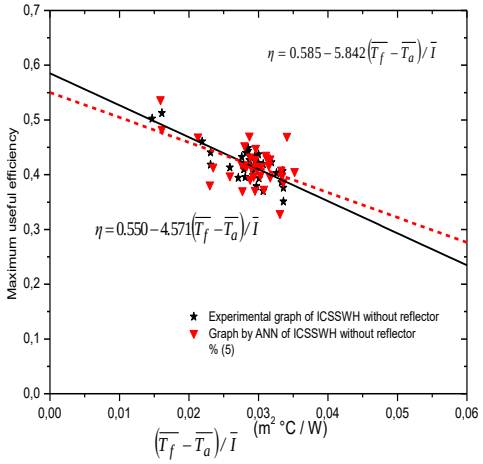

Figure 11. Characteristic graph experimental and by the ANN model of ICSSWH without reflector

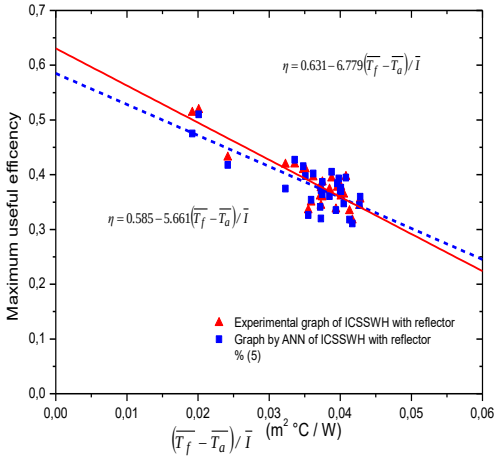

Figure 12. Characteristic graph experimental and by the ANN model of ICSSWH with reflector.

Figures 11 and 12 present a comparison between the experimental and neural method results. It is noteworthy that the models developed using the neural method is highly satisfactory, despite a slight difference observed between the curves. This slight difference indicates a small variation between the coefficients of heat loss calculated experimentally and those computed by the neural network. Overall, the neural network-based approach demonstrates good accuracy in capturing the sensor's thermal characteristics.

Table 3 provides a comprehensive summary of the thermal and optical characteristics of the two ICSSWH systems, one with a reflector and the other without a reflector. The data is obtained through both experimental methods and the ANN model. Upon analysis of this table, it becomes evident that there is a good agreement between the results obtained from the two methods used. Furthermore, the presence of the reflector has a positive impact on the performance of the ICSSWH system, as indicated by the improvement in its thermal and optical characteristics.

Table 3. Thermal and optical performance of ICSSWH for the two series of tests

Test	MUE equation	
	Experimental temperatures	**Predicted temperatures by ANN model**
ICSSWH With reflector and with insulator	$\eta = 0.631 - 6.779\left(\overline{T_f} - \overline{T_a}\right)/\bar{I}$ $\overline{K}F_E\eta_0 = 0.631$ $F_E U_L$ = 6.779 W/m²°C F_E = 0.979 U_L = 6.924 W/m²°C	$\eta = 0.585 - 5.661\left(\overline{T_f} - \overline{T_a}\right)/\bar{I}$ $\overline{K}F_E\eta_0 = 0.585$ $F_E U_L$ = 5.661 W/m²°C F_E = 0.979 U_L = 5.782 W/m²°C
ICSSWH Without reflector and without insulator	$\eta = 0.585 - 5.842\left(\overline{T_f} - \overline{T_a}\right)/\bar{I}$ $\overline{K}F_E\eta_0 = 0.585$ $F_E U_L$ = 5.842 W/m²°C F_E = 0.979 U_L = 5.967 (W/m²°C)	$\eta = 0.550 - 4.571\left(\overline{T_f} - \overline{T_a}\right)/\bar{I}$ $\overline{K}F_E\eta_0 = 0.550$ $F_E U_L$ = 4.571 W/m²°C F_E = 0.979 U_L = 4.669 W/m²°C

To compute the night-time heat loss coefficient, data is collected between sunset and sunrise of the next day. For each 5 minute interval during this period, the difference between the mean water temperature and ambient temperature is calculated. The results are then averaged over a specific duration denoted as $\Delta t = t_{sunrise} - t_{sunset}$

This average $\left(\overline{T_f} - \overline{T_a}\right)$ was then divided into the temperature difference $\left(T_i - T_f\right)$ between the water initial temperature and final temperature during this time. The heat loss coefficient can be calculated as follow [13]:

$$U_L = \frac{\left(M_w C_w + M_{cs} C_{cs}\right)\left(T_i - T_f\right)}{A\,\Delta t\left(\overline{T_f} - \overline{T_a}\right)} \qquad (7)$$

Figure 13 and Table 4 present a summary of the calculation results obtained through both experimental and neural methods for the night variation of the internal energy of the ICSSWH systems (with insulation before and without prior isolation). We notice that the energy variation follows a linear formas ($y = - ax$).

Table 4. Night time thermal properties of ICSSWH for the two series of tests

Test	Equation of the storage internal energy	
	Experimental temperatures	**Predicted temperatures by ANN model**
ICSSWH Without insulator	$MC\frac{\partial T_f}{\partial t} = -5.185\left(\overline{T_f} - \overline{T_a}\right)$ $U_L A$ = 5.185 W/°C U_L = 6.10 W/m²°C	$MC\frac{\partial T_f}{\partial t} = -5.111\left(\overline{T_f} - \overline{T_a}\right)$ $U_L A$ = 5.111 W/°C U_L = 6.01 W/m²°C
ICSSWH With insulator	$MC\frac{\partial T_f}{\partial t} = -2.923\left(\overline{T_f} - \overline{T_a}\right)$ $U_L A$ = 2.923 W/°C U_L = 3.44 W/m²°C	$MC\frac{\partial T_f}{\partial t} = -2.871\left(\overline{T_f} - \overline{T_a}\right)$ $U_L A$ = 2.871 W/°C U_L = 3.38 W/m²°C

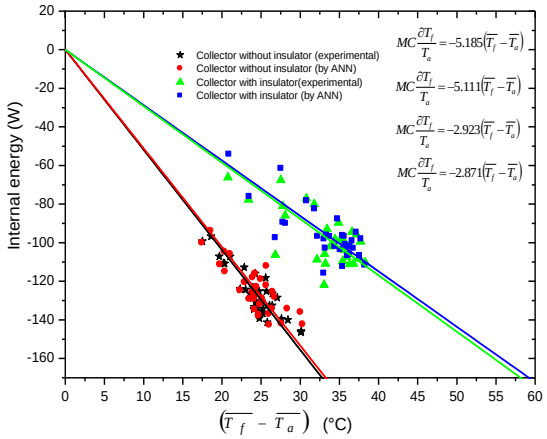

Figure 13. Internal energy variation at night of ICSSWH in the two cases experimental and neuronal.

The negative values of internal energy in Figure 13 indicate the loss of thermal energy during the night. We can see that the presence of the insulating blanket has proven effective in minimizing heat loss during this period. The agreement between the experimental and neural method results for the internal energy variation is evident from the linear pattern observed. Moreover, the results obtained from the ANN model show a significant agreement with the results obtained from the experimental. The heat loss coefficients are found to be very close, indicating good accuracy and agreement between the neural model and the experimental data.

7. Conclusion

In this study, we introduced the neural method for analyzing the performance of solar water heater. The robustness of this method was demonstrated by the excellent agreement observed between the results obtained from neural networks and experimental work. The findings of this research underscore the significance of the reflector, as it has substantially enhanced the performance of the sensor-storer by concentrating solar radiation onto the collector surface. Moreover, it serves as an insulating blanket during the night, effectively reducing heat loss during that period. The combined effects of the reflector have contributed to improved overall efficiency and performance of the solar water heater system.

Nomenclature

A_c	Total system surface area, m^2
$AADT_i$	Average Absolute Deviation
$AARDT_i$	Average Absolute Relative Deviation
$ASRDT_i$	Average Square Relative Deviation
b	bias
C_{cs}	Heat capacity of empty collector–storage unit, J kg^{-1} $°C^{-1}$
C_w	Heat capacity of water, J kg^{-1} $°C^{-1}$
F_E	System enthalpy retrieval factor,
I	Solar irradiance on collector aperture, W m^2
K	Collector incidence angle modifier,
M_{cs}	Mass of empty collector storage unit, kg
M_w	Mass of water in storage, kg
s_i	Output neuron

Greek letters

η_o	Collector optical efficiency
η	Maximum useful efficiency (MUE)

Subscripts

ANN	Artificial neural network
BRBP	Bayesian regularization back propagation
FFBP	Feed forward back propagation
ICSSWH	Integrated collector-storage solar water heater
MUE	Maximum Useful Efficiency

t	Time, s
T	Temperature of water in storage, °C
T_1	Temperature of the first tank
T_2	Temperature of the second tank
T_3	Temperature of the third tank
T_4	Temperature of the fourth tank
T_a	Room temperature, °C
$Tcal$	Temperature calculated by ANN
$Texp$	Experimental Temperature
T_f	Temperature of water in storage at sunset, °C
T_i	Temperature of water in storage at sunrise, °C
U_L	Heat loss coefficient, W m^{-1} $°C^{-1}$
w_i	Synaptic weights of neuron
x_i	Input of the neuron

References

[1] Kalogirou, S.A., Panteliou, S., 1999. A. Dentsoras, Artificial neural network used for the performance prediction of a thermosiphon solar water heater. Renewable Energy, 8:87-99.

[2] Kalogirou, S.A., 2004. Optimization of solar systems using artificial neural-networks and genetic algorithm. Applied Energy, 77:383-405.

[3] Kalogirou, S.A., 2006. Prediction of flat-plate collector performance parameters using artificial neural networks. Solar Energy, 80:248-259.

[4] Sözen, A., Menlik, T., Ünvar, S., 2008. Determination of efficiency of flat-plate solar collectors using neural network approach. Expert Systems with Applications, 35:1533-1539.

[5] Kalogirou, S.A., Lalot, S., Florides, G., Desmet, B., 2008. Development of a neural network based fault diagnostic system for solar thermal applications. Solar Energy, 82:164-172.

[6] Souliotis, M., Kalogirou, S., Tripanagnostopoulos, Y., 2009. Modelling of an ICS solar water heater using artificial neural networks and TRNSYS. Renewable Energy, 34(5): 1333-1339. [doi:10.1016/j.renene.2008.09.007]

[7] Esen, H., Ozgen, F., Esen, M., Sengur, A., 2009. Artificiel neural network and wavelet neural network approaches for modelling of a solar air heater. Expert systems with Applications, 36(8): 11240-11248.

[8] Boudries, K.R., Khellaf, A., 2003. Estimation de la Production de l'Hydrogène Solaire au Sud Algérien. Rev. Energ. Ren. : ICPWE, 73-77 (in French).

[9] MEM, 2008. Ministère de l'Énergie et des Mines. Algérie, (http://www.mem-algeria.org). (in French).

[10] Bliss, R.W., 1959. The derivation of several "plate-efficiency factors" useful in the design of flatplate solar heat collectors. Solar Energy, 3(4):55-64. [doi:10.1016/0038-092X(59)90006-4]

[11] American Society of heating, 1978. Methods of Testing to Determine the Thermal Performance of Solar Collectors, Report No. 93-77, Refrigerating and Air-Conditioning Engineers, New York.

[12] Faiman, D., 1984. Towards a Standard Method for Determining the Efficiency of Integrated Collector-Storage Solar Water Heaters. Solar Energy, 33:459-463. [doi:10.1016/0038-092X(84)90199-3]

[13] Faiman, D., Haim, H., Laufer, I., 2001. Reducing the Heat Loss at Night from Solar Water Heaters of the Integrated Collector-Storage Variety. Solar Energy, 71:87-93. [doi:10.1016/S0038-092X(01)00021-4]

[14] Abdi, H., Gahgah, M., 2003. Expérimentation d'un capteur auto stockeur compose de quatre cuves et équipé par un réflecteur. Rapport d'activité interne, SEES/MS (in French).

[15] Hassani, D., Hanini, S., Daoud K., Mauret, E., 2008. Application of the neuronal method for calculating the axial dispersion in the beds fixed of the linings parallelepipedic. Journal of Applied Sciences, 8(19): 3380-3388. [doi: 10.3923/jas.2008.3380.3388]

[16] Hassani, D., Hanini, S., 2010. Application of the neuronal method for calculating the axial dispersion in fixed beds of the spherical linings. Journal of Applied Sciences, 10(10): 823-830. [doi: 10.3923/jas.2010.823.830]

[17] Si-Moussa, C., Hanini, S., Derriche, R., Bouhedda, M., Bouzidi, A., 2008. Prediction of high-pressure vapor liquid equilibrium of six binary systems, carbon dioxide with six esters, using an artificial neural network model. Brazilian Journal of Chemical Engineering, 25: 183-199. [doi: 10.1590/S0104-66322008000100019]